Single-particle excitations in the normal state of the negative-U Hubbard model

1994 J. Phys.: Condens. Matter 6 5839

(http://iopscience.iop.org/0953-8984/6/30/007)

J. Phys.: Condens. Matter 6 (1994) 5839–5858. Printed in the UK

Single-particle excitations in the normal state of the negative-U Hubbard model

S V Traven†
Department of Physics, University of Warwick, Coventry CV4 7AL, UK

Received 17 January 1994, in final form 28 March 1994

Abstract. One-particle properties of the normal state of a negative-U Hubbard model are analysed within the framework of the incoherent local-pair (ILP) approach. In the self-consistent Hartree–Fock approximation an analytic expression for the critical value $U_c < 0$ of the coupling strength is obtained below which the system becomes unstable towards the formation of incoherent local pairs. The single-particle excitation spectrum for different regimes of the attraction strength U and particle concentration n is investigated, and the U–n phase diagram is discussed.

1. Introduction

Local pairing of fermions, mostly as an alternative model of superconductivity, has been known for decades since the pre-BCS theory suggestion of Schafroth and co-workers [1]. One of the principal features of such a theory is the existence of bound pairs of fermions above the superconducting transition temperature T_c. Studies of the ground-state properties and low-lying excitations of local-pair superconductors in the limit of strong attraction between fermions have been carried out by several authors. Thus, Leggett [2], Nozières and Schmitt-Rink [3] and Micnas and co-workers [4] found that for temperatures above the Bose condensation temperature T_c and below the pair-breaking temperature T_p the system behaves as a hard-core Bose gas on a lattice with a charge $2e$. The relevance of such a 'local-pair' superconducting mechanism to superconductivity in real compounds, including high-temperature metal-oxide superconductors, has also been studied in depth with respect to the specific nature of the attraction between fermions. Thus, Alexandrov and co-workers [5, 6] proposed a bipolaron theory of superconductivity with an attraction between electrons arising from a strong electron–phonon interaction. Mott [7] also suggested a bipolaron model of superconductivity in which the effective electron–electron attraction is induced by the exchange of magnons. The simplest form of the model Hamiltonian for such theories is that suggested by Hubbard [8]:

$$\hat{H} = -\mu \sum_{i\sigma} c_{i\sigma}^{\dagger} c_{i\sigma} - \sum_{ij\sigma} t_{ij}\, c_{i\sigma}^{\dagger} c_{j\sigma} + \frac{U}{2} \sum_{i\sigma} c_{i\sigma}^{\dagger} c_{i\sigma} c_{i-\sigma}^{\dagger} c_{i-\sigma} \tag{1}$$

where we assume an attractive interaction between electrons ($U < 0$). In (1) t_{ij} denotes the fermion hopping integral and μ is the chemical potential. A negative U in (1) obviously favours double occupancy of sites, thus leading to local-pairing effects. A version of this

† Permanent address: Moscow Engineering Physics Institute, 31 Kashirskoe sh., Moscow, 115409, Russia.

0953-8984/94/305839+20$19.50

Hamiltonian was used to describe a static binding effect at localized centres in amorphous semiconductors [9, 10] and charge-ordering phenomena [11, 12]. The model was also considered by several authors in connection with superconductivity [4].

So far, the major interest in studying the Hamiltonian in (1) has been concerned with its ground-state properties and low-lying excitations. In the weak-coupling limit the problem is that of a BCS-type theory, where the Hartree–Fock mean-field approach works well at temperatures well below some degeneracy temperature which is of the order of the Fermi energy. In the opposite limit of strong attraction the problem is reduced to that of an effective pseudo-spin Hamiltonian

$$\hat{H}_{\text{eff}} = -\sum_{ij} J_{ij}(S_i^+ S_j^- - S_i^z S_j^z) - B\sum_i (2S_i^z + 1) \tag{2}$$

with an effective 'exchange interaction' $J_{ij} = 4t_{ij}^2/|U|$, external 'magnetic field' $B = \mu + |U|/2$, and magnetization fixed by the equation for the chemical potential:

$$\frac{1}{N}\sum_i \langle S_i^z \rangle = \frac{n-1}{2}$$

where n is the number of electrons per lattice site. Then the mean-field approach can be used [4], provided one considers the system below the Bose-condensation temperature of effective 'bosons':

$$T \leqslant T_c \sim t^2/U \tag{3}$$

where t denotes the hopping integral in (1). In both limits a fairly complete analysis of the ground-state properties and the low-energy excitations has been given [4], including an interpolation between two regimes [3, 13].

For the normal state an interpolation procedure was suggested recently by Gyorffy and co-workers [14] on the basis of the hypothesis that the thermal disorder of the normal state in the presence of local pairs can be described with the help of a local-pairing amplitude

$$\langle c_{i\uparrow} c_{i\downarrow} \rangle = \frac{1}{U}\Delta e^{i\theta_i}. \tag{4}$$

Here θ_i may be interpreted as a fluctuating 'phase' of the local-pair wavefunction on the site i. In contrast to the BCS approach for low temperatures, where all the phases θ_i are coherent (which reflects the fact that the pairs are overlapping, thus forming a Bose condensate) in the ILP state the phases θ_i are entirely incoherent, fluctuating randomly, so we do not have pairs with definite momenta but a definite number of such pairs on a site. As was shown in [14], the superconducting transition in this approach may be described as a disorder–order transition. The study of such a transition in the ILP state for various coupling strengths U revealed a nice interpolation for T_c between the weak-coupling (BCS) and strong-coupling (Bose-condensate) limits, suggesting that the ILP may be thought of as of a good interpolation scheme for the description of the normal state of the system. Application of the ILP model to the calculation of such observable effects as gaps in the density of states and their detection in photoemission and tunneling measurements was discussed by Park and Joynt [15].

The purpose of the present paper is to analyse the one-particle excitation spectrum of the ILP state for various values of the coupling strength U and particle concentration n. The rest of the paper is organized as follows. In section 2 we derive general equations

for a single-particle Green function of the ILP state in the coherent potential approximation (CPA), using a single-site static method, employed for the model by the authors of [14]. In section 3 we investigate an instability of a system of fermions, interacting via a model potential in (1), towards the ILP state formation in a dilute limit and obtain the critical value for the effective attraction between fermions in our model Hamiltonian, (1), at which the instability may occur. The general solution of the ILP equations for the one-electron coherent potential $\Sigma(z)$ is given in section 4. We analyse our ILP equations for various values of the pairing potential Δ and chemical potential μ and discuss three different regimes: (i) small pairing potential Δ, when the single-particle excitation spectrum contains no local gap; (ii) the one-particle excitation spectrum has a gap, corresponding to the binding of electrons into local pairs, although with only a finite fraction of electrons forming local pairs; (iii) the strong-coupling (atomic) regime, in which all the fermions in the system are bound into the local pairs. We analyse the single-particle excitation spectrum for all of these different regimes of U and n, and calculate the ILP state U–n phase diagram in the zero-temperature limit. Conclusions then follow in section 5.

2. Single-particle Green function of the ILP state in the coherent potential approximation

To obtain information on the single-particle excitation spectrum of our system, described by the Hamiltonian in (1) in the presence of the local-pairing amplitude in (4) we use the method of random fields, applied to the problem at hand by Gyorffy and co-workers [14]. We shall work with the Nambu-style matrix Green function [16]:

$$\underline{G}(i, j; \tau) \equiv -\mathrm{i}\,\langle \hat{c}_i(\tau); \hat{c}_j^{\dagger}(0)\rangle \qquad \hat{c}_i(\tau) = \begin{bmatrix} c_{i\uparrow}(\tau) \\ c_{i\downarrow}^{\dagger}(\tau) \end{bmatrix}. \tag{5}$$

The matrix elements of this Green function are

$$\underline{G}(i, j; \tau) = -\mathrm{i} \begin{Bmatrix} \langle c_{i\uparrow}(\tau); c_{i\uparrow}^{\dagger}(0)\rangle & \langle c_{i\uparrow}(\tau); c_{i\downarrow}(0)\rangle \\ \langle c_{i\downarrow}^{\dagger}(\tau); c_{i\uparrow}^{\dagger}(0)\rangle & \langle c_{i\downarrow}^{\dagger}(\tau); c_{i\downarrow}(0)\rangle \end{Bmatrix}. \tag{6}$$

Here $\langle \ldots; \ldots\rangle$ denotes Wick's time-ordering followed by averaging in a thermal ensemble. As usual, we expand the Green function in (5) into a Fourier series. The sum over the Matsubara fermion frequencies is

$$\underline{G}(i, j; \tau) = \frac{\mathrm{i}}{\beta} \sum_n \underline{G}(i, j; \omega_n) \mathrm{e}^{-\mathrm{i}\omega_n \tau} \qquad \omega_n = \mathrm{i}\,\frac{(2n+1)\pi}{\beta}.$$

In the method of random fields [14] we have the following equation for the Green function of an electron in a random potential:

$$\sum_l \begin{Bmatrix} (\omega_n + \mu - U n_{i\downarrow})\,\delta_{il} + t_{il} & \Delta_i\,\delta_{il} \\ \Delta_i^*\,\delta_{il} & (\omega_n - \mu + U n_{i\uparrow})\,\delta_{il} - t_{il} \end{Bmatrix} \underline{G}(l, j; \omega_n) = \underline{1}\,\delta_{ij} \tag{7}$$

where n_i and Δ_i are the independent random variables.

The qualitatively different feature of the theory is the fluctuating pairing potential Δ_i, which is a complex number:

$$\Delta_i = |\Delta_i| \mathrm{e}^{\mathrm{i}\theta_i}.$$

We assume in the following that only the θ_i phase fluctuates and will accept for the other independent variable $n_{i\sigma}$ its Hartree–Fock values: $n_{i\sigma} \equiv \bar{n}_\sigma$, so that the only role of the corresponding terms in (7) will be the renormalization of the chemical potential μ:

$$\mu = \tilde{\mu} + \tfrac{n}{2}U. \tag{8}$$

Here and in the following the absence of spin fluctuations is assumed. We shall also drop the 'tilde' in (8) until we pay particular attention to the Hartree–Fock correction. Equation (7) is a generalization of the corresponding Gor'kov equations [17, 18] for a particular configuration of $n_{i\sigma}$ and Δ_i. One should mention that such combinations of the Gor'kov equations and the method of random fields have been discussed previously by several authors with the application to the theory of superconducting alloys [19]. However, in contrast with the problem of superconductivity in transition-metal alloys, where the external disorder makes it sensible to consider fluctuations of magnitude of both n_i and Δ_i, the present model, which deals with the normal state of the system in the absence of the external disorder, takes into account only the thermal disorder resulting in fluctuations of phases θ_i.

One can now rewrite (7) in the ordinary form for a Dyson equation:

$$\underline{G} = \underline{G}_0 + \underline{G}_0 \underline{V} \underline{G} \tag{9}$$

where the matrix of the random potential is

$$\underline{V}_i = \begin{bmatrix} 0 & -\Delta_i \\ -\Delta_i^* & 0 \end{bmatrix}. \tag{10}$$

The central feature of the CPA method is the approximation for the ensemble averaged Green function:

$$\langle \underline{G}(i, j; \omega_n) \rangle_a \tag{11}$$

by $\underline{G}^c$, which describes the Green function for the CPA effective medium. We will not discuss here the CPA method itself, so that the reader should refer to [14] and to the review by Elliott and co-workers [20] for the details. Here we only briefly note that the average Green function $\underline{G}^c$ in (11) describes the motion of an electron on a non-random effective lattice. The corresponding Dyson equation for our effective medium Green function $\underline{G}^c$ has the following matrix form:

$$\underline{G}^c = \underline{G}_0 + \underline{G}_0 \underline{\Sigma} \underline{G}^c. \tag{12}$$

Here $\underline{\Sigma}^i(\omega_n)$ is the frequency-dependent complex coherent potential at site i. In the following we shall consider only the homogeneous limit, so that we will assume that the coherent potential is independent of the lattice site: $\underline{\Sigma}^i(\omega_n) \equiv \underline{\Sigma}(\omega_n)$. If we now consider an 'impurity' in this effective lattice at site i, described by the potential in (10), it is easy to show with the help of the Dyson equations, (9) and (12), that the corresponding 'impurity' Green function takes the form

$$\underline{G}^{\theta_i}(i, i; \omega_n) = \{\underline{1} - \underline{G}^c(i, i; \omega_n)[\underline{V}_i - \underline{\Sigma}^i(\omega_n)]\}^{-1} \underline{G}^c(i, i; \omega_n). \tag{13}$$

Then, according to the CPA, we must proceed with the averaging procedure in (11):

$$\int \mathrm{d}\theta_i \, P(\theta_i) \, \underline{G}^{\theta_i}(i, i; \omega_n) = \underline{G}^c(i, i; \omega_n). \tag{14}$$

Here we will take for the 'probability distribution' $P(\theta_i)$ that of randomly disordered incoherent local pairs and assume in the homogeneous limit [14]

$$\Delta_i = \Delta e^{i\theta_i} \tag{15}$$

$$P(\theta_i) = \frac{1}{2\pi}. \tag{16}$$

With such a $P(\theta_i)$ the CPA condition in (11) for the impurity Green function of (13) is

$$\frac{1}{2\pi}\int_0^{2\pi} d\theta_i \, \underline{D}^{\theta_i}(i,i;\omega_n) = \underline{1}. \tag{17}$$

Here

$$\underline{D}^{\theta_i}(i,i;\omega_n) = \{1 - \underline{G}^c(i,i;\omega_n)[\underline{V}_i - \underline{\Sigma}(\omega_n)]\}^{-1}.$$

The CPA average Green function

$$\underline{G}^c(i,i;\omega_n) = \sum_k^{BZ} \underline{G}^c(k;\omega_n) \tag{18}$$

can be obtained from its Dyson equation, (12):

$$\begin{Bmatrix} \omega_n - \varepsilon_k - \Sigma_{11}(\omega_n) & -\Sigma_{12}(\omega_n) \\ -\Sigma_{21}(\omega_n) & \omega_n + \varepsilon_k - \Sigma_{22}(\omega_n) \end{Bmatrix} \underline{G}^c(k,\omega_n) = \underline{1}. \tag{19}$$

Here $\varepsilon_k = \varepsilon_k^0 - \mu$, and ε_k^0 denotes the 'bare' band energy. In the state with Δ_i and $P(\theta_i)$ described by (15) and (16), the off-diagonal elements of the matrices $\underline{G}^c$ and $\underline{\Sigma}$ vanish because of local gauge invariance. Moreover, in the absence of magnetism the one-particle Green function must be independent of the spin projection: $G_{\sigma\sigma} = G_{-\sigma-\sigma}$. For the matrix elements of our Nambu-style Green function $\underline{G}^c$ and those of the coherent potential $\underline{\Sigma}$ this implies

$$G_{22}^c(i,i;\omega_n) = -G_{11}^c(i,i;-\omega_n) \qquad \Sigma_{22}(\omega_n) = -\Sigma_{11}(-\omega_n).$$

Using the notation

$$G(\omega_n) \equiv G_{11}^c(i,i;\omega_n) \qquad \Sigma(\omega_n) \equiv \Sigma_{11}(\omega_n)$$

we arrive at the following equation for the 'impurity' Green function in (13):

$$\underline{G}^{\theta_i}(i,i;\omega_n) = \frac{1}{\mathrm{DET}} \begin{Bmatrix} G(\omega_n)[1 + G(-\omega_n)\,\Sigma(-\omega_n)] & G(\omega_n)\,G(-\omega_n)\,\Delta e^{i\theta_i} \\ G(\omega_n)\,G(-\omega_n)\,\Delta e^{-i\theta_i} & -G(-\omega_n)[1 + G(\omega_n)\,\Sigma(\omega_n)] \end{Bmatrix} \tag{20}$$

where

$$\mathrm{DET} \equiv -[1 + G(\omega_n)\,\Sigma(\omega_n)][1 + G(-\omega_n)\,\Sigma(-\omega_n)] - \Delta^2 G(\omega_n) G(-\omega_n).$$

Now the basic CPA equation, derived from (17), takes the following form:

$$G(\omega_n) = -\frac{\Sigma(-\omega_n)}{\Delta^2 + \Sigma(\omega_n)\,\Sigma(-\omega_n)}. \tag{21}$$

To determine the pairing potential Δ and the chemical potential μ we must impose the self-consistency conditions, which follow from the definition of the Green function in (6):

$$\Delta e^{i\theta_i} = iUG^{\theta_i}_{12}(i,i;t \to +0) = -\frac{U}{\beta}\sum_n G^c_{12}(i,i;\omega_n)e^{-i\omega_n\epsilon} \tag{22}$$

$$\frac{n}{2} = -i\,G^c_{11}(i,i;t \to -0) = \frac{1}{\beta}\sum_n G^c_{11}(i,i;\omega_n)e^{i\omega_n\epsilon}. \tag{23}$$

Here ϵ is a positive infinitesimal. Using (20) for the impurity Green function and (21) for the CPA Green function we have, instead of (22) and (23):

$$\frac{1}{\beta}\sum_n \frac{\Sigma(\omega_n)\Sigma(-\omega_n)}{\Delta^2 + \Sigma(\omega_n)\,\Sigma(-\omega_n)}e^{-i\omega_n\epsilon} = -\frac{\Delta^2}{U} \tag{24}$$

$$\frac{1}{\beta}\sum_n \frac{\Sigma(-\omega_n)}{\Delta^2 + \Sigma(\omega_n)\,\Sigma(-\omega_n)}e^{i\omega_n\epsilon} = -\frac{n}{2}. \tag{25}$$

To complete the system of equations we must now provide a recipe for the calculation of the CPA Green function in (19). Making an analytic continuation for the Fourier coefficients $\underline{G}(\omega_n)$ and $\underline{\Sigma}(\omega_n)$ from the complex points ω_n into the complex z-plane with the cut along the real z-axis, we have for the CPA Green function in the complex z-plane:

$$\underline{G}^c(z) = \int_{-W/2-\mu}^{W/2-\mu} d\varepsilon\,\rho_0(\varepsilon)\begin{bmatrix} 1/(z-\varepsilon-\Sigma(z)) & 0 \\ 0 & 1/(z+\varepsilon+\Sigma(-z)) \end{bmatrix}. \tag{26}$$

Following [14], we shall employ a model density of states $\rho_0 = \text{constant}$, given by

$$\rho_0(\varepsilon) = \frac{1}{2} \times \begin{cases} 1 & |\varepsilon+\mu| \leqslant 1 \\ 0 & \text{otherwise.} \end{cases} \tag{27}$$

Here, and in the subsequent analysis, we will measure all energies in the units of half bandwidth, i.e. $W/2$. Then the calculation of the integral in (26) is trivial and for the analytic continuation of the Green function $G(z)$ we have

$$G(z) = \coth^{-1}[z - \Sigma(z) + \mu] \equiv \frac{1}{2}\ln\left(\frac{z-\Sigma(z)+\mu+1}{z-\Sigma(z)+\mu-1}\right). \tag{28}$$

It is assumed in (28) that above and below the real axis the appropriate branch of the complex logarithm function is taken (both $\Sigma(z)$ and $G(z)$ must have negative imaginary parts in the upper half-plane of the complex variable z, and positive parts below the real axis):

$$\coth^{-1}(x \pm iy) \equiv \frac{1}{2}\coth^{-1}\left(\frac{x^2+y^2+1}{2x}\right) \mp \frac{i}{2}\cot^{-1}\left(\frac{x^2+y^2-1}{2y}\right). \tag{29}$$

Now our fundamental CPA equation, (21), is reduced to the equation on the coherent potential $\Sigma(z)$:

$$\coth^{-1}[z-\Sigma(z)+\mu]=-\frac{\Sigma(-z)}{\Delta^2+\Sigma(z)\,\Sigma(-z)}. \tag{30}$$

Since the essential physics, as far as the single-particle excitations is concerned, is contained in the frequency-dependent self-energy $\Sigma(\omega)$ which is a discontinuity of $\Sigma(z)$ across the cut

$$\Sigma(\omega)\equiv \mathrm{i}[\Sigma(\omega+\mathrm{i}0)-\Sigma(\omega-\mathrm{i}0)]$$

our purpose will be the calculation of $\Sigma(z)$ just near the real axis, i.e. for $z=\omega\pm\mathrm{i}0$:

$$\Sigma(\omega\pm\mathrm{i}0)=\mathrm{Re}\,[\Sigma(\omega)]\mp\mathrm{i}\frac{\Gamma(\omega)}{2}\qquad \Gamma(\omega)\geqslant 0 \tag{31}$$

and, using (29), we have, instead of (30), a system of four coupled equations for $\mathrm{Re}\,[\Sigma(\pm\omega)]$, $\Gamma(\pm\omega)$. For the given density n and the attraction strength U the self-consistent solutions for Δ and μ are then determined from the following equations (where the sums over the Matsubara frequencies have been converted into contour integrals):

$$\frac{1}{2\pi\mathrm{i}}\oint_{\Gamma_0}\frac{\Sigma(z)\,\Sigma(-z)}{\Delta^2+\Sigma(z)\Sigma(-z)}\frac{\mathrm{d}z}{\mathrm{e}^{-\beta z}+1}=\frac{\Delta^2}{U} \tag{32}$$

$$\frac{1}{2\pi\mathrm{i}}\oint_{\Gamma_0}\frac{\Sigma(-z)}{\Delta^2+\Sigma(z)\Sigma(-z)}\frac{\mathrm{d}z}{\mathrm{e}^{\beta z}+1}=-\frac{n}{2} \tag{33}$$

with a suitably chosen contour Γ_0. Since, as we shall see in the next section, the integrands do not have poles in the complex z-plane, except those of the function

$$f^{\pm}(z)=\frac{1}{\mathrm{e}^{\mp\beta z}+1}$$

the contour Γ_0 in the integrals of (32) and (33) runs over the cut branches along the real z-axis, where both $G(z)$ and $\Sigma(z)$ have a discontinuity across the cut. Thus we obtain the single-particle excitation spectrum described by $\Sigma(\omega)$ for some particular interaction strength and particle concentration. We shall realize this programme in section 4.

3. Analytic analysis of the ILP instability

Before discussing the properties of the general solution for the one-electron coherent potential we investigate our equation for $\Sigma(z)$ in (30) in the limiting cases of small and large values of the pairing potential Δ, where the equations can be handled analytically, and where a physical interpretation at low densities is straightforward.

3.1. Threshold for the ILP instability

To discover conditions under which the instability towards incoherent local-pair formation occurs in systems of fermions with the model interaction between the particles given by the Hamiltonian in (1), we consider the limit $\Delta \to 0$, when one can expect that the properties of our system are those of a normal metal with a small concentration of 'impurities': thermally disordered local pairs. The effect produced by this weak disorder may be taken into account using a standard perturbation theory method [21]. To second order in the 'perturbation' potential Δ the self-energy correction due to the interaction with these charge fluctuations is given by

$$\Sigma_0(z) \simeq -\Delta^2 G_0(-z). \tag{34}$$

This corresponds to the single-site self-energy diagram in the 'non-crossing' approximation. To obtain the 'pair-breaking' temperature T_p (which is different, of course, from the superconducting temperature T_c), i.e. the temperature at which a non-trivial solution for Δ appears, one should substitute $\Sigma_0(z)$, (34), into the equation for the pairing potential in (32). In the limit $\Delta \to 0$ the corresponding equation for the transition temperature T_p is then

$$1 + \frac{U}{\beta_p} \sum_n G_0(\omega_n)\, G_0(-\omega_n) = 0 \tag{35}$$

where $\beta_p \equiv 1/T_p$. If we now proceed with the calculation of the Matsubara sum in (35) by converting it into the contour integral as in (32), we obtain the following equation for T_p:

$$\frac{1}{U} = -\frac{1}{\pi} \int_0^{+\infty} \mathrm{Im}\,[G_0(\omega + \mathrm{i}0) G_0(-\omega - \mathrm{i}0)] \tanh\left(\frac{\beta_p \omega}{2}\right) \mathrm{d}\omega \tag{36}$$

where the Green function of the ideal Fermi-system with our model density of states, given by (27), has the form

$$G_0(\omega + \mathrm{i}0) = \coth^{-1}(\omega + \mu + \mathrm{i}0) = \frac{1}{2} \begin{cases} \ln\left(\dfrac{1+\omega+\mu}{1-\omega-\mu}\right) - \mathrm{i}\pi & |\omega + \mu| < 1 \\ \ln\left(\dfrac{\omega+\mu+1}{\omega+\mu-1}\right) & |\omega + \mu| > 1. \end{cases} \tag{37}$$

Besides the ILP transition temperature, (36) also contains some useful information about the critical value of the attractive potential U at which the instability may occur. Indeed, performing the integration in (36) in the limit $T_p \to 0$, we obtain for the critical interaction strength

$$U_c = -\frac{1}{\ln 2} \tag{38}$$

so that $U_c \simeq -1.44$. Note that for the case of two fermions such attraction would correspond to a bound state with a radius of about an interatomic distance. Such a strong interaction will obviously lead to a breakdown of the Fermi-liquid-like picture for the system. To demonstrate this let us now assume the situation when a weak instability ($\Delta \ll 1$) has developed for the interaction strength just below U_c and analyse what effect it has on the

one-electron spectrum. In the dilute limit when $\varepsilon_F \simeq 1+\mu \simeq n \ll 1$, where n is the fermion concentration, we can estimate the low-temperature one-electron retarded self-energy near the Fermi-surface from (37) as

$$\Sigma_0(0) \simeq -\frac{\Delta^2}{2}\ln\left(\frac{n}{2}\right) - i\frac{\pi}{2}\Delta^2. \tag{39}$$

The self-energy correction $\mathrm{Re}[\Sigma_0(0)]$ to the bare band energy is positive because of the Pauli exclusion principle. Indeed, since some fraction of the lattice sites are doubly occupied, the average electron energy should increase. For the relaxation rate due to scattering by thermally disordered local pairs we have from the imaginary part of (39):

$$\frac{1}{\tau_i} = -2\mathrm{Im}[\Sigma_0(0)] \simeq \pi\,\Delta^2. \tag{40}$$

We should emphasize at this point that the non-zero imaginary part of Σ does not imply a 'breakdown' of the Fermi-liquid theory, since the ILP state is essentially a finite-temperature approach, dealing with temperatures above the superconducting transition temperature T_c.

The further increase of the interaction strength (and, correspondingly, Δ) will lead to a more dramatic change of the spectrum. Indeed, at some critical Δ the real part of our self-energy, (39) becomes of the order of the Fermi-energy:

$$\Delta_0^2 \simeq -2\frac{n}{\ln(n/2)} \tag{41}$$

and the one-electron spectrum displays instability towards a gap formation at $\omega = 0$, as will be shown in section 4.

3.2. ILP state in the strong-coupling (atomic) limit

Another limit of the model where our equations have analytic solutions is that of a large coupling strength U, for which we could expect a situation in which all the fermions are bound into the local pairs. In this regime the one-particle spectrum must have a gap, separating two 'Hubbard' subbands (the lower one corresponding to the electron states participating in the pairs formation, and the upper one describing the electron–hole excitations), each with a half-width of the order of unity, as that of the bare electron band. If one neglects such an 'infinitesimal' on the scale of characteristic energies, which are of the order of the coupling strength U, our Green function in (28) can be expanded for the large values of the argument:

$$\coth^{-1}[z - \Sigma(z) + \mu] \simeq \frac{1}{z + \mu - \Sigma(z)}. \tag{42}$$

Then, using our basic equation for the coherent potential (30), we get the following solution for $\Sigma(z)$ and the Green function $G(z)$:

$$\Sigma(z) = \frac{\Delta^2}{z - \mu} \tag{43}$$

$$G(z) = \frac{z - \mu}{z^2 - z_0^2} \tag{44}$$

with $z_0 = \sqrt{\Delta^2 + \mu^2}$ which has the obvious meaning of half the binding energy of a local pair. With $\Sigma(z)$ and $G(z)$ in (43) and (44) the integration in (32) and (33) is trivial, so that we arrive at the following results for the pairing amplitude Δ and the chemical potential μ:

$$\frac{|U|}{2\sqrt{\Delta^2+\mu^2}} \tanh\left(\frac{\sqrt{\Delta^2+\mu^2}}{2T}\right) = 1 \tag{45}$$

$$\mu = -\frac{|U|}{2}(1-n). \tag{46}$$

The 'boson' chemical potential, which is twice that of the fermion value, does not depend on temperature. This fact is well understood, since there is no entropy associated with motion of the bosons, as they are entirely incoherent. Moreover, the 'true' chemical potential must take into account the Hartree–Fock term (8), so that of the bosons equals $-U$. The temperature dependence of the pairing potential Δ which follows from (45) is due to the electron–hole pairs' excitations. For low temperatures, we have for the pairing amplitude Δ and the one-electron 'binding' energy z_0

$$\Delta = |U|\sqrt{\frac{n}{2}\left(1-\frac{n}{2}\right)} \tag{47}$$

$$z_0 = \frac{|U|}{2} \tag{48}$$

so that the energy needed to destroy a pair is $2z_0 \equiv |U|$. Clearly, since the effective boson annihilation and creation operators are given by the expressions $b_i \equiv c_{i\uparrow}c_{i\downarrow}$ and $b_i^\dagger \equiv c_{i\downarrow}^\dagger c_{i\uparrow}^\dagger$, respectively, it follows from (22) that the average number of bosons is equal to

$$\overline{N}_b = \left(\frac{\Delta}{U}\right)^2. \tag{49}$$

For a small enough density of fermions we thus have from (47) for the average number of bosons half of that the fermions, i.e. *all* existing fermions are bound into the pairs.

The poles of the Green function (44) correspond to the centres of two 'Hubbard' subbands, where one-particle excitations are situated. As mentioned above the lower band must correspond to bound electrons. Indeed, for the self-energy in the lower band we have

$$\Sigma(z = -z_0) = -|U|(1 - \tfrac{n}{2})$$

so it is determined by the attractive potential of another electron with a positive correction due to the Pauli exclusion principle. For an electron in the upper band only the last term survives:

$$\Sigma(z = z_0) = |U|\frac{n}{2}.$$

The pole of the self-energy, (43), seems to be an intrinsic feature of the strong-coupling regime. Generally speaking, the existence of a pole in $\Sigma(z)$, where the one-electron Green function vanishes, is normally associated with superconductivity [18]. In the present approach, in which we do not consider long-range order, we interpret this state as the extreme Bose limit, when *all the existing electrons* are bound into incoherent local pairs. Note, that our approximation for the strong-coupling regime which leads to the expansion of the Green function, (42), is valid until the pole of $\Sigma(z)$ in (43) is positioned far away from the top of the lower 'Hubbard' subband, i.e. $|\mu| \leqslant z_0 - 1$. This means that the pairing potential should be sufficiently large: $\Delta^2 \geqslant 2|\mu|$.

4. General solution for the single-particle self-energy

In this section we discuss solutions of our fundamental equation for the one-electron coherent potential $\Sigma(z)$, (30), for arbitrary Δ and μ. As was clearly demonstrated in the previous section, the corresponding solution for Σ must display different behaviour for different regimes of the coupling strength. Our purpose now is to study how and where (for which Δ and μ) the crossover occurs and what are the spectral properties of the corresponding one-particle Green functions.

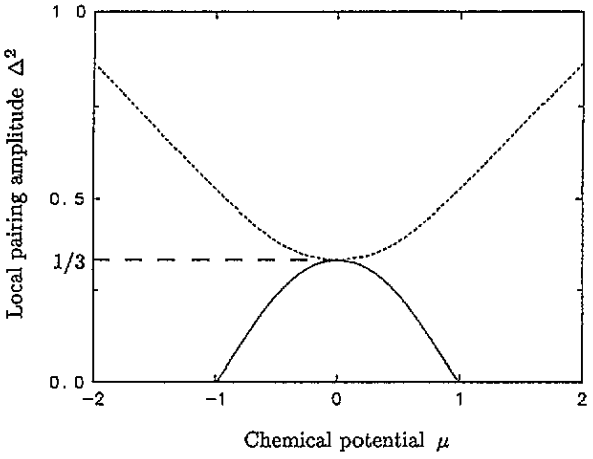

Figure 1. The ILP state Δ^2–μ phase diagram. The full curve displays the critical values of Δ^2 at which the ILP state one-particle spectrum becomes unstable towards gap formation. For values of $\Delta^2(\mu)$ above the broken curve the one-particle self-energy contains a pole, located between two 'Hubbard' subbands.

We have solved our basic equation, (30), for different values of Δ and μ, having reduced the equation for $\Sigma(z)$ near the real axis $z = \omega \pm i0$ to a system of four differential equations for four real functions. The latter was solved numerically using the standard methods. Mathematical details of the corresponding solution are described in appendix A, and here we will discuss only the results. Spectral properties of the system are analysed in terms of the quasi-particle density of states (DOS) which is given by the following equation:

$$\rho(\omega) \equiv -\frac{1}{\pi} \operatorname{Im}[G(\omega + i0)]. \tag{50}$$

As follows from the analysis given in appendix A, for small values of the pairing potential Δ (those lying under the full curve of figure 1) the one-particle excitation spectrum contains only one band with a non-zero density of states at $\omega = 0$. An example of such a single-band spectrum is plotted in figure 2 for the following parameters: $\Delta^2 = 0.05$ and $\mu = -0.7$. This range of Δ may be thought of as a limit with the small concentration of local pairs, so that one may expect that the properties of the system are close to those of a normal metal with some effective disorder produced by the existing local pairs. Indeed, figure 2 illustrates that the corresponding solution for $\Sigma(\omega)$ closely resembles the form given by (34). The real part of the one-electron self-energy at $\omega = 0$ is positive, indicating the influence of the Pauli exclusion principle on an electron moving in a system with charge fluctuations: the incoherent local pairs. Note that the quasi-particle density of states for this set of parameters which is plotted in figure 5(*a*) contains no gap at $\omega = 0$.

The one-electron spectrum has a single-band character only for $\Delta^2(\mu)$ lying below the full curve shown in figure 1. For $|\mu| \to 1$ this curve, as shown in appendix A, has the

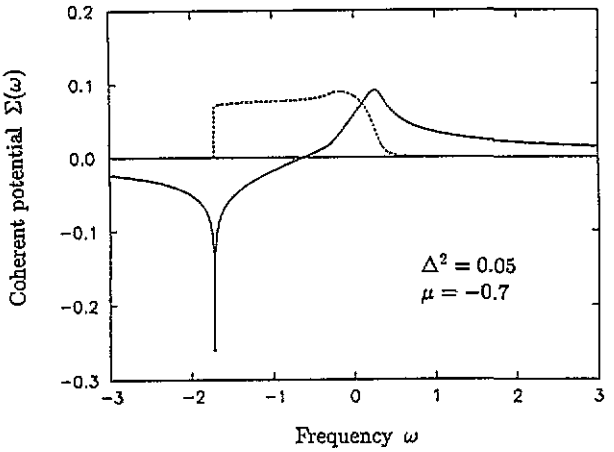

Figure 2. The one-particle self-energy in the weak-coupling regime. Real (full curve) and imaginary (broken curve) parts of the coherent potential $\Sigma(\omega + i0)$ as functions of frequency for $\Delta^2 = 0.05$ and $\mu = -0.7$.

following asymptotic behaviour:

$$\Delta_0^2(\mu \to \pm 1) \simeq -2\frac{1-|\mu|}{\ln(1-|\mu|)} \tag{51}$$

which corresponds to small concentrations of either electrons or holes. At densities near half-filling, the curve $\Delta_0^2(\mu)$ approaches the critical value

$$\Delta_0^2(\mu \to 0) = \frac{1}{3}. \tag{52}$$

Note that (51), which corresponds to the dilute regime, is equivalent to that discussed in section 3, i.e. (41). For $\Delta(\mu) \geqslant \Delta_0(\mu)$ the one-electron spectrum is split into two subbands, so that to add an electron to the system one needs an energy larger than μ. As an illustration of the two-band single-particle spectrum we plot in figure 3 the corresponding solutions for $\Sigma(\omega)$ for $\Delta^2 = 0.3$ and $\mu = -0.8$ ($\rho(\omega)$ for this set of parameters is plotted in figure 5(*b*)). An interesting feature of $\Sigma(\omega)$ in this range of parameters is that part of the occupied electron states (i.e. those lying below $\omega = 0$) have positive self-energy (the real part of the complex potential is positive: $\mathrm{Re}\,\Sigma(\omega) > 0$). One can interpret these electron states as those corresponding to the electrons not bound to the local incoherent pairs but strongly affected by the interaction with pair fluctuations. Such a type of solution for $\Sigma(\omega)$ corresponds to the values $\Delta^2(\mu)$ which lie *above* the full curve but *below* the broken curve shown in figure 1. The corresponding set of equations which provide the solution for $\Delta_1^2(\mu)$ is given by (A18)–(A20).

If we now move to higher values of Δ, which lie above the broken curve $\Delta_1^2(\mu)$ in figure 1, we will have to deal with the strong-coupling limit. As an example of such a regime we plot in figure 4 the solution of our basic equation for $\Sigma(\omega)$ (with the density of states $\rho(\omega)$ given by figure 5(*c*)) for $\Delta^2 = 1$ and $\mu = -0.7$. The main feature of the corresponding solution for $\Sigma(\omega)$ in this range of parameters is the existence of a pole between two 'Hubbard' subbands at a frequency ω_0 given by a solution of (A17) in appendix A. The presence of that pole leads to a positive $\mathrm{Re}[\Sigma]$ in the upper band and to a negative $\mathrm{Re}[\Sigma]$ in the lower one. This implies an effective attractive potential for all electrons in the occupied electron states, thus making one think of all the electrons in the system as bound into incoherent local pairs. We associate this ILP state with the extreme Bose limit.

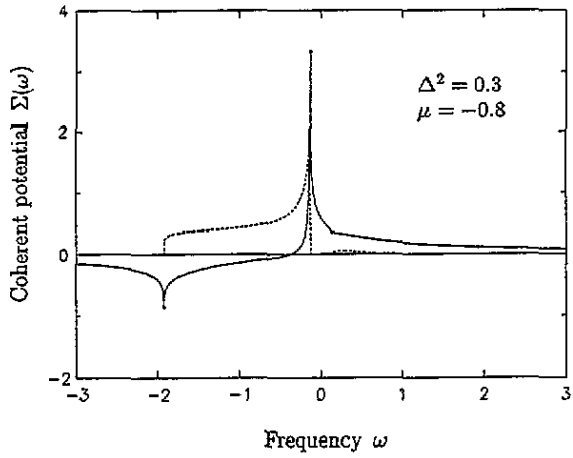

Figure 3. The one-particle self-energy in the intermediate-coupling regime. Real (full curve) and imaginary (broken curve) parts of the coherent potential $\Sigma(\omega + i0)$ as functions of frequency for $\Delta^2 = 0.3$ and $\mu = -0.8$.

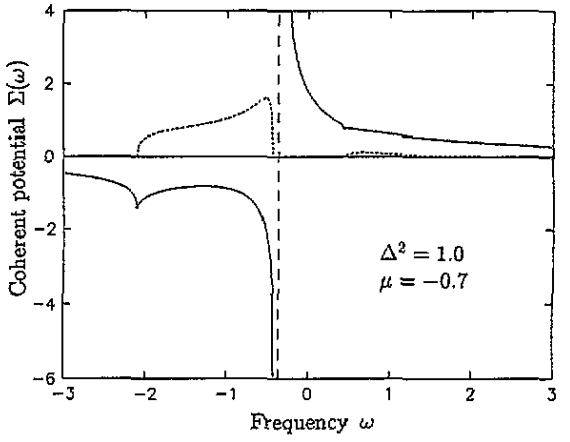

Figure 4. The one-particle self-energy in the strong-coupling regime. Real (full curve) and imaginary (broken curve) parts of the coherent potential $\Sigma(\omega + i0)$ as functions of frequency for $\Delta^2 = 1.0$ and $\mu = -0.7$. Note that a pole of $\mathrm{Re}[\Sigma]$ appears for these values of Δ^2 and μ.

Since we have now obtained the numerical solution for $\Sigma(\omega \pm i0)$, we can evaluate the integrals (32) and (33) to obtain the 'phase separating' curves on the U–n plane, which would correspond to those of $\Delta_0^2(\mu)$ (full curve) and $\Delta_1^2(\mu)$ (broken curve) in figure 1. Indeed, the contour integration in (32) and (33) is now reduced to that along the real z axis:

$$\frac{1}{\pi}\int_0^{+\infty} \mathrm{Im}\,\frac{\Sigma(\omega + i0)\Sigma(-\omega - i0)}{\Delta^2 + \Sigma(\omega + i0)\Sigma(-\omega - i0)} \tanh\left(\frac{\omega\beta}{2}\right) d\omega = -\frac{\Delta^2}{U} \tag{53}$$

$$\frac{1}{\pi}\int_{-\infty}^{+\infty} \mathrm{Im}\,\frac{\Sigma(-\omega - i0)}{\Delta^2 + \Sigma(\omega + i0)\Sigma(-\omega - i0)} \frac{d\omega}{e^{\beta\omega} + 1} = \frac{n}{2}. \tag{54}$$

We calculated the corresponding phase diagram in zero-temperature limit using U and n evaluated from the integrals in (53) and (54). Figure 6 displays the results of this calculation with the full curve corresponding to the transition from the single-band case to the two-band case (full curve $\Delta_0(\mu)$ in figure 1) and the broken curve being the result, related to the curve $\Delta_1(\mu)$ in figure 1 (broken curve).

We have also evaluated the relative fraction of local pairs from (49). The result for low densities is shown in figure 7. It clearly displays the features of the 'weak-' and strong-coupling regimes discussed above. Indeed, as can be seen from figure 7, only a small part

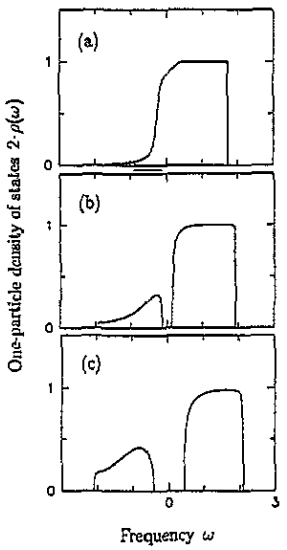

Figure 5. One-particle density of states for different values of Δ and μ. (*a*) 'Weak'-coupling regime: $\Delta^2 = 0.05$ and $\mu = -0.7$. (*b*) Intermediate-coupling regime: $\Delta^2 = 0.3$ and $\mu = -0.8$. (*c*) Strong-coupling regime: $\Delta^2 = 1.0$ and $\mu = -0.7$.

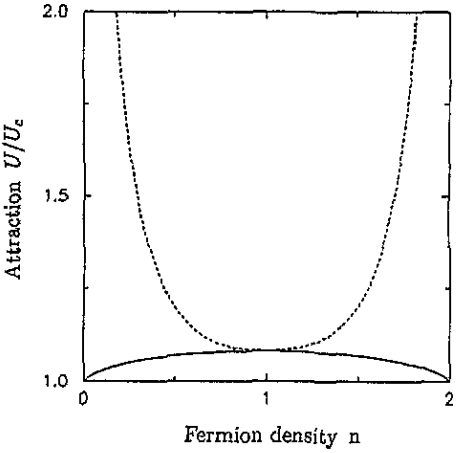

Figure 6. The ILP state U–n phase diagram. The full curve displays the transition into the 'two-band' regime with a gap in the one-particle density of states. The broken curve indicates a crossover between the intermediate- and strong-coupling ('Bose-gas') limits.

of fermions form incoherent local pairs as the coupling strength exceeds some critical value $U_0(n)$ (full curve in figure 6). The broken curve in figure 7 shows the 'boson' fraction as calculated along the other critical curve $U_1(n)$ (the broken curve in figure 6). It is clearly seen from that result that, for attractions stronger than $U_1(n)$, the system is in the extreme Bose limit, so that the effective number of 'bosons' is just half of that of fermions:

$$\overline{N}_b \simeq \frac{n}{2}.$$

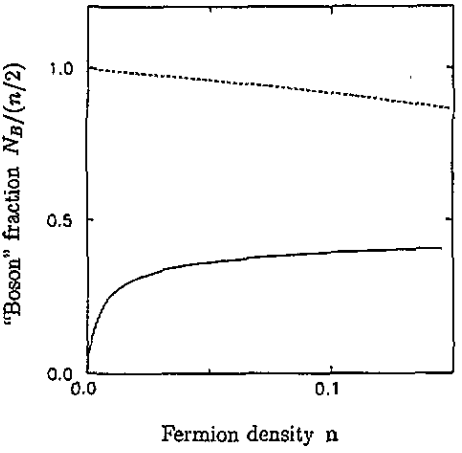

Figure 7. Relative fraction of 'bosons' at low concentrations. The two curves show 'boson' density, (49), relative to half the total fermion concentration, calculated along the 'phase-separation' curves shown in figures 1 and 5. The full curve displays the fraction of 'bosons', calculated for the values of Δ^2 and μ at which a gap appears in the excitation spectrum. The broken curve corresponds to that in figure 6.

This analysis of the phase diagrams is, of course, only of qualitative significance, since we calculated the corresponding quantities at $T = 0$, and the ILP state is essentially the high-temperature ($T \gg T_c$) phase. However, the reasonable results we get, for example for the effective 'boson' density in the strong-coupling limit, imply that the method, at least in the mean-field approach, correctly takes into account the existence of the bound states. The further verification of the ILP phase could probably be obtained by a study of the transport properties of the system since, as was mentioned in the introduction, one of the main features of the local-pair theory is the existence of charge carriers with charge $2e$ in the normal state.

5. Conclusion

We have studied single-particle excitations in the incoherent local-pair (ILP) state of the negative-U Hubbard model [14] for various regimes of the coupling strength U and particle concentration n. It was shown that with the attraction between electrons exceeding some critical value, $U_c = -1/\ln 2$, the system of fermions described by the Hamiltonian (1) becomes unstable towards formation of the incoherent local pairs—thermally disordered pairs of fermions. This approach is valid in the temperature range

$$T_c \ll T \ll T_p$$

(where T_c is the Bose-condensation temperature, and T_p is the pair-breaking temperature).

Within the framework of the ILP model [14], and using the formalism of the coherent potential approximation (CPA), we have solved the equation for the one-electron coherent potential in a thermally disordered crystal for arbitrary values of the pairing amplitude Δ and the chemical potential μ.

We have demonstrated for the limit of a small concentration of local pairs ($|U| \sim |U_c|$) that in this case the properties of the ILP state are similar to those of a normal metal, although $\Sigma(\omega)$ has a non-zero imaginary part at $\omega = 0$. In the strong-coupling regime ($|U| \gg |U_c|$) we have shown that the system displays the properties of a Bose liquid with all the existing fermions bound into the local pairs. In the intermediate regime the system may be considered as an ionization equilibrium of local pairs and strongly correlated electrons.

We have investigated spectral properties of the one-electron Green function using the general solution of the CPA equation for the complex coherent potential $\Sigma(z)$ and obtained single-particle excitation spectra for various regimes of the coupling strength and particle concentration. Results of the general solution are consistent with both the weak- and strong-coupling regimes.

We have also evaluated the ILP state U–n phase diagram which displays the presence of three different regimes of the system's behaviour: the 'weak'-coupling regime with properties similar to those of an impure normal metal; the strong-coupling extreme Bose-limit; and the intermediate regime, which is a 'mixture' of incoherent local-pair states and highly-correlated one-electron states.

Acknowledgments

The author is grateful to A S Alexandrov and S G Rubin for the useful and helpful discussions, and, especially, to B L Gyorffy and J B Staunton for their continuous interest in this work, and for valuable comments and remarks. The author also acknowledges financial support from the Royal Society.

Appendix A. Solution of the CPA equation on $\Sigma(z)$

To investigate (30) let us consider two functions of the complex variable z just above the real axis:

$$\Sigma(z) = \begin{cases} \Sigma_1(z) & \mathrm{Re}\,(z) > 0 \\ \Sigma_2(-z) & \mathrm{Re}\,(z) < 0. \end{cases} \tag{A1}$$

According to the analytic properties of $\Sigma(z)$ we have for $z = \omega + \mathrm{i}0$

$$\Sigma_1 \equiv S_1 - \mathrm{i}\gamma_1 \tag{A2}$$

$$\Sigma_2 \equiv S_2 + \mathrm{i}\gamma_2 \tag{A3}$$

with non-negative γ_1 and γ_2. Using (29), we can then rewrite our general equation on $\Sigma(z)$, equation (30), in the form of four equations for S_1, S_2, γ_1 and γ_2:

$$\frac{1}{4}\ln\left(\frac{(\omega+\mu-S_1+1)^2+\gamma_1^2}{(\omega+\mu-S_1-1)^2+\gamma_1^2}\right) = -\frac{S_1(S_2^2+\gamma_2^2)+S_2\Delta^2}{(\Delta^2+S_1S_2+\gamma_1\gamma_2)^2+(S_1\gamma_2-S_2\gamma_1)^2} \tag{A4}$$

$$\frac{1}{4}\ln\left(\frac{(\omega-\mu+S_2+1)^2+\gamma_2^2}{(\omega-\mu+S_2-1)^2+\gamma_2^2}\right) = \frac{S_2(S_1^2+\gamma_1^2)+S_1\Delta^2}{(\Delta^2+S_1S_2+\gamma_1\gamma_2)^2+(S_1\gamma_2-S_2\gamma_1)^2} \tag{A5}$$

$$\frac{1}{2}\cot^{-1}\left(\frac{(\omega+\mu-S_1)^2+\gamma_1^2-1}{2\gamma_1}\right) = \frac{\gamma_1(S_2^2+\gamma_2^2)+\gamma_2\Delta^2}{(\Delta^2+S_1S_2+\gamma_1\gamma_2)^2+(S_1\gamma_2-S_2\gamma_1)^2} \tag{A6}$$

$$\frac{1}{2}\cot\left(\frac{(\omega-\mu+S_2)^2+\gamma_2^2-1}{2\gamma_2}\right) = \frac{\gamma_2(S_1^2+\gamma_1^2)+\gamma_1\Delta^2}{(\Delta^2+S_1S_2+\gamma_1\gamma_2)^2+(S_1\gamma_2-S_2\gamma_1)^2}. \tag{A7}$$

In the case of half-filling, i.e. when $\mu = 0$, it is easy to show that the solution $\Sigma(z)$ of (30) is antisymmetric:

$$\Sigma(-z) \equiv -\Sigma(z). \tag{A8}$$

Provided we have such additional symmetry in our equations, leading to that of functions (A2) and (A3):

$$S_1(\omega) \equiv -S_2(\omega) \equiv S(\omega) \tag{A9}$$

$$\gamma_1(\omega) \equiv \gamma_2(\omega) \equiv \gamma(\omega) \tag{A10}$$

our system, equations (A4)–(A7), reduce to that for two functions $S(\omega)$ and $\gamma(\omega)$. The general solution of the system, (A4)–(A7), for non-negative ω with $\gamma_1, \gamma_2 > 0$ gives $\Sigma(\omega + \mathrm{i}0)$. It is instructive to start an investigation of the properties of such a solution from an analysis of the region of ω, where the one-particle density of states is non-zero, as is the imaginary part of Σ. To determine the points ω_1 and ω_2 (and, as follows from (A4)–(A7), $-\omega_1$ and $-\omega_2$, respectively) at which the quasi-particle density of states vanishes, one has to consider the limit $\gamma_1, \gamma_2 \to 0$ in (A4)–(A7). A straightforward calculation shows that this leads to the following equation for the real parts S_1 and S_2:

$$\begin{vmatrix} \left(\dfrac{S_2}{\Delta^2+S_1S_2}\right)^2 - \sinh^2\left(\dfrac{S_2}{\Delta^2+S_1S_2}\right) & -\left(\dfrac{\Delta}{\Delta^2+S_1S_2}\right)^2 \\ -\left(\dfrac{\Delta}{\Delta^2+S_1S_2}\right) & \left(\dfrac{S_1}{\Delta^2+S_1S_2}\right)^2 - \sinh^2\left(\dfrac{S_1}{\Delta^2+S_1S_2}\right) \end{vmatrix} = 0 \tag{A11}$$

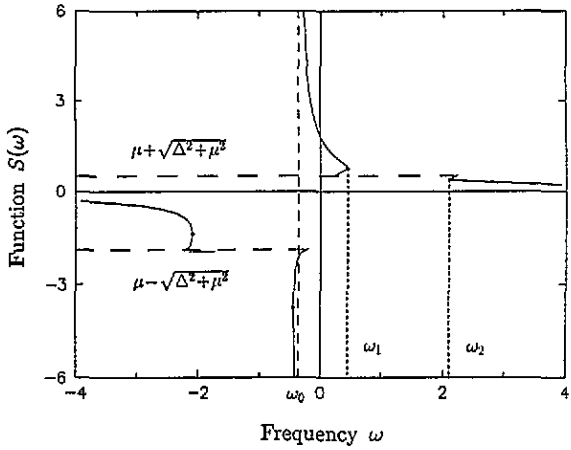

Figure A1. Real roots of $S(\omega)$. The four branches correspond to all real roots of (A12) and (A13) for $\Delta^2 = 1.0$ and $\mu = -0.7$. Full circles shows 'critical' points where $(dS/d\omega) \to \infty$, corresponding to the edges of the one-particle spectrum. As clearly seen from the plot, $S(\omega)$ as a function of ω has a pole for these Δ^2 and μ.

with S_1 and S_2 being given by the corresponding solutions of the equations:

$$S_1 - \mu - \omega = \coth\left(\frac{S_2}{\Delta^2 + S_1 S_2}\right) \tag{A12}$$

$$S_2 - \mu + \omega = \coth\left(\frac{S_1}{\Delta^2 + S_1 S_2}\right). \tag{A13}$$

The solution of three coupled equations, (A11)–(A13), thus give frequencies ω at which the one-particle density of states vanishes, so they are nothing but the 'band edges'. As can be easily shown, mathematically our condition for such ω, equation (A11), is equivalent to that for ω at which derivatives of two functions $S_1(\omega)$ and $S_2(\omega)$, as *purely real* solutions of (A12) and (A13), go to infinity:

$$\left(\frac{dS_{1,2}}{d\omega}\right) \to \infty. \tag{A14}$$

To illustrate this fact we plot in figure 7 all the real roots of (A12) and (A13) for $\Delta^2 = 1$ and $\mu = -0.7$. The corresponding function $S(\omega)$ has four branches with the following starting points shown in figure 7:

$$S = \mu + \sqrt{\Delta^2 + \mu^2} \qquad \text{at} \qquad \omega = \sqrt{\Delta^2 + \mu^2} \pm 1$$

and

$$S = \mu - \sqrt{\Delta^2 + \mu^2} \qquad \text{at} \qquad \omega = -\sqrt{\Delta^2 + \mu^2} \pm 1.$$

Circles (also displayed in figure A1) on each branch mark points at which our condition for $\gamma_1, \gamma_2 \to 0$, equation (A11), is satisfied, thus determining the edges of the one-particle spectrum. As clearly seen from figure A1, the quasi-particle 'bands' are placed between the derivative singularities of the real function $S(\omega)$, where $(dS/d\omega) \to \infty$, just as we mentioned above. For our example, shown in figure A1, we have two 'Hubbard bands', located below and above $\omega = 0$, i.e. in the intervals $(-\omega_2, -\omega_1)$ and (ω_1, ω_2), correspondingly. Here, and in what follows, we will assume that ω_1 and ω_2 are solutions of (A14) ($\omega_2 > \omega_1$). In order to find the frequencies ω_1 and ω_2 for any given Δ and μ we have to solve the corresponding equations, (A11)–(A13), which can be done in the general case only numerically.

Let us discuss now what are the different regimes of our one-particle spectra for various Δ^2 and μ. A straightforward analysis of the condition in (A14) shows that we will have two subbands, i.e. $\omega_1 > 0$ only if $\Delta(\mu)$ exceeds some critical value $\Delta_0(\mu)$ given by the following system of equations:

$$\left(\frac{\Delta}{\Delta^2+S_0^2}\right)^2 = \sinh^2\left(\frac{S_0}{\Delta^2+S_0^2}\right) - \left(\frac{S_0}{\Delta^2+S_0^2}\right)^2 \tag{A15}$$

$$S_0 - \mu = \coth\left(\frac{S_0}{\Delta^2+S_0^2}\right). \tag{A16}$$

Here $S_0 \equiv S_1(\omega = 0) \equiv S_2(\omega = 0)$ is the real root of (A1) at which the condition (A14) is satisfied. The corresponding numerical solution $\Delta^2(\mu)$ is plotted in figure 1 (full curve). For the values Δ less than $\Delta_0(\mu)$ the one-particle density of states contains only one 'band', so that there is no gap in the single-particle excitation spectrum. For Δ larger than $\Delta_0(\mu)$ the one-particle density of states is split into two subbands, thus leading to a gap in the excitation spectrum.

As revealed by a further analysis of (A11)–(A13), in the strong-coupling regime ($\Delta^2 \gg \mu \gg 1$) the solution $S(\omega)$ has a simple pole located away from quasi-particle bands, at a frequency given by the following equation:

$$\left(1 - \frac{(\omega+\mu)(\omega-\mu)}{\Delta^2}\right)\tanh\left(\frac{\omega+\mu}{\Delta^2}\right) = -\frac{\omega+\mu}{\Delta^2} \tag{A17}$$

where the non-trivial solution ($\omega \neq -\mu$) should be taken. As the pairing amplitude decreases, the pole approaches one of the subbands and crosses it at some value $\Delta_1(\mu)$ which can be obtained from the equations

$$3\left(\frac{\Delta^2}{S_1}\right)^2 + 1 = S_1^2 \sinh^2\left(\frac{1}{S_1}\right) \tag{A18}$$

$$2\omega_1 = \frac{\Delta^2}{S_1} + S_1 - \coth\left(\frac{1}{S_1}\right) \tag{A19}$$

$$\omega_1 - \mu = \frac{\Delta^2}{S_1}. \tag{A20}$$

Here ω_1 and S_1 are the 'band edge' and the value $S_1(\omega_1)$ at this point, respectively. The solution $\Delta_1(\mu)$ can be obtained from this system numerically and is plotted in figure 1 (broken curve). Note that the parameters $\Delta^2 = 0.05$ and $\mu = -0.7$ for the example in figure A1 correspond to the region of $\Delta^2(\mu)$ above the critical curve $\Delta_1^2(\mu)$ in figure A1.

As the region where complex (with non-zero imaginary part) solutions for Σ_1 and Σ_2 lie is determined we can employ some numerical method to find them. We calculated our four functions, i.e. real (S_1 and S_2) and imaginary (γ_1 and γ_2) parts of Σ_1 and Σ_2 by numerical solution of a corresponding system of differential equations on $\Sigma_1(\omega)$ and $\Sigma_2(\omega)$. That can be obtained from either (A4)–(A7), or (A12) and (A13). In the latter case, assuming that Σ_1 and Σ_2 are complex, we have

$$\left(\frac{d\Sigma_1}{d\omega}\right)\left[\left(\frac{\Sigma_2}{\Delta^2+\Sigma_1\Sigma_2}\right)^2[(\omega-\mu-\Sigma_1)^2-1]-1\right]$$

$$-\left(\frac{d\Sigma_2}{d\omega}\right)\left(\frac{\Delta}{\Delta^2+\Sigma_1\Sigma_2}\right)^2[(\omega-\mu-\Sigma_1)^2-1]=-1 \tag{A21}$$

$$\left(\frac{d\Sigma_2}{d\omega}\right)\left[\left(\frac{\Sigma_1}{\Delta^2+\Sigma_1\Sigma_2}\right)^2[(\omega-\mu+\Sigma_2)^2-1]-1\right]$$
$$-\left(\frac{d\Sigma_1}{d\omega}\right)\left(\frac{\Delta}{\Delta^2+\Sigma_1\Sigma_2}\right)^2[(\omega-\mu+\Sigma_2)^2-1]=1. \tag{A22}$$

After substitution of (A2) and (A3) into (A21) and (A22) we obtain a system of four differential equations. We solved these equations using the standard fourth-order Runge–Kutta method with the starting point ω_0 lying in the middle of the interval (ω_1, ω_2), i.e.

$$\omega_0=\frac{\omega_1+\omega_2}{2} \tag{A23}$$

where in the 'one-band' case we take $\omega_1=0$. The initial values for $S_1(\omega_m)$, $S_2(\omega_m)$, $\gamma_1(\omega_m)$ and $\gamma_2(o_m)$ were obtained from the system (A4)–(A7) using a minimization procedure. In the case of $\mu=0$, one can determine the 'starting point' of integration without such a minimization. Indeed, it can be shown from (A4)–(A7) (after the substitution (A9) and (A10)), that then we can use as a starting point either $\omega_0=0$ for the one-band case, when the pairing amplitude is less than the critical value given by $\Delta^2=1/3$, or frequency ω_0 at which condition $S(\omega_0)=\omega_0$ holds. In the former case we have for the starting point ω_0

$$S(\omega_0)=0$$

and $\gamma(\omega_0)$ is to be determined from the following equation:

$$\frac{\gamma}{\Delta^2+\gamma^2}=\tan^{-1}\left(\frac{1}{\gamma}\right).$$

In the opposite limit, i.e. the two-band case, the starting point $S(\omega_0)=\omega_0$ is determined from the equation

$$\Delta^2=\omega_0^2+\gamma^2$$

where $\gamma=\gamma(\omega_0)$ is a solution of

$$\frac{1}{2\gamma}=\tan^{-1}\left(\frac{1}{\gamma}\right).$$

The properties of the complex solutions of our equations for $\Sigma(\omega)$, (A4)–(A7), are discussed in section 4.

References

[1] Schafroth M R, Blatt J M and Butler S T 1957 *Helv. Phys. Acta* **30** 93
[2] Leggett A J 1980 *Modern Trends in the Theory of Condensed Matter* ed J Przswystawa (Berlin: Springer)
[3] Nozières P and Schmitt-Rink S 1985 *J. Low Temp. Phys.* **59** 195
[4] Micnas R, Ranninger J and Robaskiewicz S 1990 *Rev. Mod. Phys.* **62** 1
[5] Alexandrov A S and Ranninger J 1981 *Phys. Rev.* B **23** 1796; 1981 *Phys. Rev.* B **24** 1164

[6] Alexandrov A S, Ranninger J and Robaszkiewicz S 1986 *Phys. Rev.* B **33** 4526
[7] Mott N F 1990 *Adv. Phys.* **39** 55
[8] Hubbard J 1963 *Proc. R. Soc.* A **276** 238; 1964 *Proc. R. Soc.* A **277** 237; 1964 *Proc. R. Soc.* A **281** 401
[9] Anderson P W 1975 *Phys. Rev. Lett.* **34** 953
[10] Street R A and Mott N F 1975 *Phys. Rev. Lett.* **35** 1293
[11] Ionova G V, Makarov E F and Ionov S P 1977 *Phys. Status Solidi* b **81** 671
[12] Lubimov V S *et al* 1976 *Phys. Status Solidi* b **75** 91
[13] Randeria M, Duan J-M and Shieh L-Y 1989 *Phys. Rev. Lett.* **62** 981
[14] Gyorffy B L, Staunton J B and Stocks G M 1991 *Phys. Rev.* B **44** 5190
[15] Park K A and Joynt R 1993 *Phys. Rev.* B **48** 16833
[16] Nambu Y 1960 *Phys. Rev.* **117** 648
Eliashberg G M 1960 *Zh. Eksp. Teor. Fiz.* **38** 966 (Engl. Transl. 1960 *Sov. Phys.–JETP* **11** 696)
[17] Parks D R 1969 *Superconductivity* vol 1, ed D R Parks (New York: Dekker)
[18] Abrikosov A A, Gor'kov L P and Dzyaloshinskii I E 1963 *Methods of Quantum Field Theory in Statistical Physics* (Englewood Cliffs, NJ: Prentice-Hall)
[19] Lustfeld H 1973 *J. Low Temp. Phys.* **12** 595
Kerker G and Bennemann K H 1974 *Solid State Commun.* **14** 399
Weinkauf A and Zittartz J 1975 *J. Low Temp. Phys.* **18** 229
[20] Elliott R J, Krumhansl J A and Leath P L 1974 *Rev. Mod. Phys.* **46** 465
[21] Abrikosov A A and Gor'kov L P 1959 *Zh. Eksp. Teor. Fiz.* **36** 319 (Engl. Transl. 1960 *Sov. Phys.–JETP* **11** 696)